Marcello BIANCHINI

IMPROVED SCALAR INTENSITY MEASURES IN PERFORMANCE-BASED EARTHQUAKE ENGINEERING

Nota Tecnica n. 215

Anno 2008

UNIVERSITÀ DEGLI STUDI DI BOLOGNA

DISTART
Dipartimento di Ingegneria, delle Strutture, dei Trasporti,
delle Acque, del Rilevamento, del Territorio

Viale Risorgimento, 2 – 40136 Bologna

SUMMARY

An earthquake intensity measure (IM) is a characteristic of a recorded ground motion that quantifies the severity of a seismic event. In reliability analysis of structural systems subjected to ground shaking, the choice of IM plays a leading role. In probabilistic engineering assessment, the IM is used both as a scale factor for recorded ground motions in incremental dynamic analysis and as that parameter which defines the seismic hazard at a specified site. In this paper, the geometric mean of pseudo-spectral acceleration ordinates over a certain range of periods, $S_{a,avg}\left(T_1,\ldots,T_n\right)$, or briefly $S_{a,avg}$, is used as a scalar IM to predict inelastic structural response of buildings subjected to recorded ground motions. This average of spectral values is a better predictor than the elastic pseudo-spectral acceleration at fundamental period of structure, $S_a\left(T^{(1)}\right)$, especially for inelastic structural systems. Furthermore, the seismic hazard at the site in terms of $S_{a,avg}$ as IM is simpler than the one performed for vector-valued and inelastic IMs. Especially for inelastic multi-degree-of-freedom systems with long periods, $S_{a,avg}$ is very sensitive to higher-mode effects, showing a limited levels of dispersion at different given ductility levels. $S_{a,avg}$ is studied as a statistical predictor of structural response and is compared with conventional elastic and inelastic scalar IMs. The study is completed with suggestions about the period range over which the average should be calculated, the spacing periods and the necessary number of points of spectral ordinates, in order for Sa,avg to be most effective.

INTRODUCTION

Performance-Based Earthquake Engineering (PBEE, [19]) is an approach which provides a set of useful tools to support seismic risk decisions and seismic performance through a probabilistic framework. PBEE is used by both professional and academic analysts of structural systems subjected to ground shaking. The performance is measured in terms of the amount of damage sustained by a building, when affected by earthquake ground motion, and the impacts of this damage on post-earthquake disposition of the building. The concept can be extended to all structures and their supported nonstructural components and contents. While the general framework concerns all aspects of the performance based engineering (including structural and nonstructural design, construction quality assurance and maintenance of building integrity throughout its life

cycle) this paper focuses on the structural aspects of the problem, by evaluation of the inelastic response of structural buildings.

The PBEE process has been provided with a robust methodology by the Pacific Earthquake Engineering Research Center (PEER), which directly incorporates the effects of uncertainty and randomness at each step of performance assessment procedure. This methodology defines the Intensity Measure (IM) concept as that characteristic parameter of earthquake ground motion that affects the engineering demands on structural systems. Classical examples of this indicator may be the peak values of ground shaking in terms of acceleration, velocity and displacement (a.k.a., PGA, PGV and PGD), or the elastic pseudo-spectral acceleration at the fundamental period of a structure, $S_a(T^{(1)})$. However, any other parameter can be an IM if it can be expressed as a function of mean annual frequency (MAF) of exceeding of a certain level of ground motion parameter. In order to define the MAF of exceeding a certain level of IM for the area where the building is located, Probabilistic Seismic Hazard Analysis (PSHA, [16, 25]) must be carried out in terms of the selected intensity measure. After the appropriate ground motion IM has been chosen to capture important earthquake characteristics that affect building behavior, structural response can be quantified by Engineering Demand Parameters (EDPs), which are usual to predict damage to structural and nonstructural components and systems [36]. Possible choices could be maximum base shear, node rotations, peak story ductilities, various proposed damage indexes, peak roof drift, the floor peak inter-storey drift angles $\theta_1, \ldots, \theta_n$ of a n-storey structure, or their maximum, i.e., the maximum peak inter-storey drift angle, θ_{max}, defined as the peak over response time and maximum over the height of the structure. In reliability analysis, the hazard information can be combined with a certain EDP parameter prediction (given a selected IM) in order to asses the MAF of exceeding a specified value of that structural demand parameter: this link is formally expressed by Probabilistic Seismic Demand Analysis (PSDA, [29]) and represents an important task in PBEE framework. Hence, the choice of IM can affect the quality of the reliability result.

The elastic spectral acceleration has been used as a predictor and IM in seismic performance assessment [30], although significant variability in the structural response level has been observed for tall and long period buildings. The problem of *insufficiency* of $S_a(T^{(1)})$ is in part due to the fact that it does not reflect important higher mode

spectral accelerations which depend on earthquake magnitude [1]. This problem has been addressed by pairing it with a measure of spectral shape, ε, in a vector-valued IM [3], $\langle S_a(T^{(1)}), \varepsilon \rangle$. Nevertheless, in the light of PSDA approach, to a vector-valued IM must be associated a vector-valued PSHA to obtain the joint hazard curve [9], which has not yet been commonly applied, or using the conventional seismic disaggregation analysis [8]. It has been shown that the effectiveness of ε as a criterion to select ground motion records and to predict inelastic response of multi-degree-of-freedom systems is considerably greater than that of $S_a(T^{(1)})$ alone for ordinary strong ground motions. In order to provide a good predictor of inelastic structural response for those buildings located both far from and near to earthquake-source, a new scalar intensity measure based on inelastic spectral displacement, S_{di}, has been recently developed. It has been demonstrated that, for structural systems dominated by the first mode of vibration, the S_{di} predictor is more convenient than $\langle S_a(T^{(1)}), \varepsilon \rangle$, whereas, for those structures affected by higher-mode periods, it needs to be combined with a higher frequency elastic spectral displacement [24, 32].

Especially for practical applications, the difficulties in working with vector-valued or inelastic IM can be a barrier which is hard to overcome. It is well-known that structural response of MDOF or inelastic systems is sensitive to multiple periods T_i [5], so an intensity measure which averages elastic spectral acceleration values over a certain range of periods might be a useful and convenient predictor of structural response of inelastic systems. Previously, in order to assess the influence of earthquake duration on the seismic response of masonry structures, an average of spectral accelerations was considered as a strong-motion parameter [13]. By comparing different demand predictors, it was shown that correlations between damage and elastic spectral acceleration were improved by averaging the spectral ordinates over an interval which ranges from $T^{(1)}$ (i.e., the uncracked initial structural behavior) to a value approximately three times greater (i.e., the supposed damaged final stiffness), reflecting the stiffness degradation as the shaking progress. However, this range of periods was considered only for very stiff structures that do not show higher-mode effects (e.g., masonry buildings). The concept of averaging spectral acceleration values over a certain period range is already anticipated in federal provisions [22], although it is more of a rough guide based on design spectrum to choose recorded ground motions rather than to define one predictor. In fact, both for two-

and three-dimensional response history analysis procedures, many codes states that the ground motion records must be scaled such that the average value of the 5% damped response spectra for the suite of motions is not less than the design response spectrum for the site, for periods ranging from $0.2T^{(1)}$ to $1.5T^{(1)}$ [2]. Nevertheless, this choice of period range has not been formally evaluated.

The present work aims to show the effectiveness of $S_{a,avg}(T_1, \ldots, T_n)$, or briefly $S_{a,avg}$, as an intensity measure in probabilistic seismic demand assessment. The $S_{a,avg}$ IM was defined as the geometric mean of the spectral acceleration ordinates at a set of n periods, i.e., the n-th root of the product of n elastic spectral values, and it is applied here to demand assessment of inelastic single- and multi- degree-of freedom systems. It is found that $S_{a,avg}$ can be used as a useful and practical predictor of structural response, compared with other conventional intensity measures.

RESPONSE PREDICTION IN PBEE FRAMEWORK

The aim of PSDA is to assess the structural performance of a given building by probabilistic assessment of the response under ground motions of varying intensity, which is subsequently combined with information about seismic hazard at the site, calculated using PSHA, which provides the Mean Annual Frequency (MAF) of exceeding a specified level of IM value, $\lambda_{\mathrm{IM}}(im)$. Under the assumption of Poissonian occurrences, the probability that the IM random variable is greater than a certain level, im, in a certain period of time (usually 1 year), approximately matches the corresponding MAF, $P\left[\mathrm{IM} > im;\ 1 \text{ year}\right] = \lambda_{\mathrm{IM}}\left(im\right)$. This is allowed if the product between the rate of occurrence of events and the considered period of time is relatively small (less than approximately 0.1). First of all, the IM is used to quantify the ground motion hazard at a site due to seismicity in the region, e.g., through a ground motion prediction model. Hence, the feasibility of computing this seismic hazard in terms of a selected IM must be considered; properly, we speak about the *hazard computability* property of a ground motion.

In general, the EDPs are obtained through structural response simulation using the chosen intensity measures and corresponding earthquake records. One method of calculating EDPs is through nonlinear Incremental Dynamic Analysis (IDA, [33]), which predicts structural response under ground motion records incrementally scaled to dif-

ferent IM levels. A collection of IDA curves parameterized on the same IMs and EDP and generated for the the same structure under different recording defines the so-called *IDA curve set*. Then, we can define median and 16%, 84% IDA curves to summarize an IDA curve set. This is consistent also with the assumption to consider the random variable EDP (given an IM level) log-normally distributed around the mean and the standard deviation of their natural logarithms, respectively called *median* and *dispersion* [29]. By combination of the site-specific ground motion hazard curve with the structural response information, the MAF of exceeding a specified level of EDP value, $\lambda_{\mathrm{EDP}}(edp) = P[\mathrm{EDP} > edp]$, is obtained by the Total Probability Theorem [12] in the following integral formulation:

$$\lambda_{\mathrm{EDP}}(edp) = \int_{im} G_{\mathrm{EDP|IM}}(edp, im)|\mathrm{d}\lambda_{\mathrm{IM}}(im)|, \tag{1}$$

where $G_{\mathrm{EDP|IM}}(edp, im) = P[\mathrm{EDP} > edp|\mathrm{IM} = im]$ means the probability of exceeding a specified EDP level, *edp*, given a level of IM, *im*, or the complementary cumulative distribution function (CDF) of EDP given IM. Equation (1) represents the classical form of disaggregation of the MAF in terms of EDP and IM proposed in PBEE framework. However, in order to compare the "goodness" of different IMs (i.e., their influence on $\lambda_{\mathrm{EDP}}(edp)$ assessment), it is not necessary to assess the whole integral: in fact, as $\lambda_{\mathrm{IM}}(im)$ does not concern a particular building but only the site where it is located, the first integrand represents the most relevant statistical link between structural parameters and hazard measures at the site.

The first integrand in Equation (1) assumes the so-called *IM-based rule*, which provides the distribution of demand, EDP, that a given level of intensity, IM, can generate in the structure. In an IDA curve set it is hard to define a value that signals collapse for all IDA curves; in other words, prescribing a single point on the IDA curves that clearly divides them in two regions (non-collapse and collapse) does not result always feasible. This difficulty can be overcome by the *EDP-based rule*, which provides the distribution of intensities IM that are required to produce a level of damage, *edp*, or a *given ductility level*, μ. By using an EDP-based rule instead of the IM- one, the structural response hazard can be computed as:

$$\lambda_{\mathrm{EDP}}(edp) = \int_{im} F_{\mathrm{IM}_{cap}|\mathrm{EDP}}(im', edp)|\mathrm{d}\lambda_{\mathrm{IM}}(im')|, \tag{2}$$

where $F_{\mathrm{IM}_{cap}|\mathrm{EDP}}(im', edp) = P\left[\mathrm{IM}_{cap} < im' | \mathrm{EDP} = edp\right]$ is the CDF of IM capacity given EDP. This manner to express the distribution function of structural response capacity conditioned a level of IM was used in the past by several authors (e.g., [6, 7]). The random variable IM_{cap} represents the distribution of IM values resulting in the structure (i.e., the structural capacity in terms of IM), having a certain EDP level. In general, the probability of exceeding a specified level of EDP given a level of IM does not match exactly the probability of not exceeding a level of IM_{cap} fixed and EDP value. This is particularly true if we use mean and standard deviation to summarize EDP- or IM-stripes. However, it has been shown that the 16%, 50%, and 84% fractiles given IM almost perfectly match, respectively, the 84%, 50%, and 16% fractiles given EDP [34], and the results from Equations (1) and (2) will theoretically produce identical $\lambda_{\mathrm{EDP}}(edp)$ results. Again, it follows that the random variable IM_{cap} given an EDP level can be considered log-normally distributed around its own median and dispersion. Fig. 1 show the similarity between (a) IM- and (b) EDP-based rule, from a statistical point of view. The two rules are applied to an IDA curve set of 40 recorded ground motions summarized by 16%, 50% (median), and 84% fractiles. It should be noted that for the same EDP level and probability value we observe that $im \approx im'$, i.e., the two methods are indeed comparable. Owing to these considerations, in this work we use the EDP-based rule, which has the advantage of simplicity and ease of implementation, especially for performance levels other than collapse.

Furthermore, the EDP-based rule can be assumed to define statistical parameters as median, percentile and standard deviation of IDA curve set, and so assess the "goodness" of a selected IM. A good IM is structure dependent, captures higher-mode effects and inelastic behavior of buildings, and regards the frequency content of recorded ground motions. Strictly speaking, in order to ensure a reliable result of Equation (1) or (2), some features of the selected ground motion intensity measure must be provided. Here, we will focus our attention on *efficiency*, which is defined here as the standard deviation of IM values associated with a given EDP level, $\sigma_{\ln(\mathrm{IM}_{cap}|\mathrm{EDP})}$. The standard error of the sample mean of $\ln\mathrm{IM}_{cap}$ for a specified EDP level is proportional to $\sigma_{\ln(\mathrm{IM}_{cap}|\mathrm{EDP})}$ and so reducing $\sigma_{\ln(\mathrm{IM}_{cap}|\mathrm{EDP})}$ this reduces the number of nonlinear dynamic analyses and earthquake records necessary to estimate the conditional distribution of IM given EDP level with an adequately small uncertainty. As example, Fig. 2 compares two

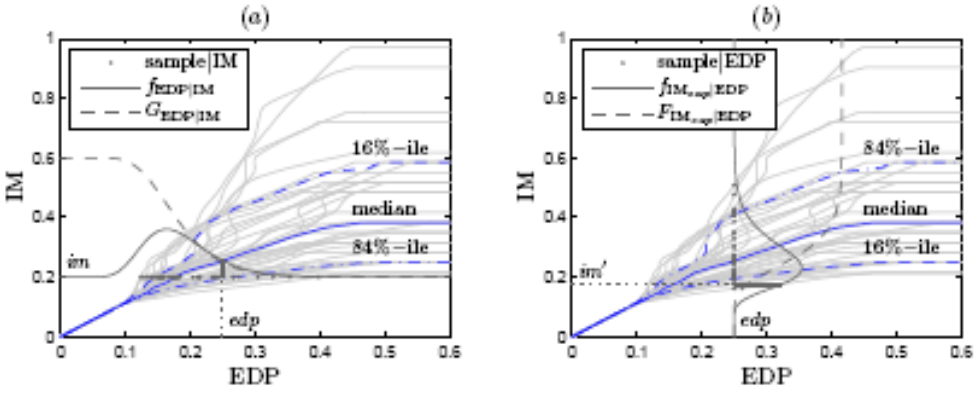

Figure 1: Distribution function for (a) IM-based rule and (b) EDP-based rule of IDA curve set constituted of a suite of 40 recorded ground motions. The area subtended by the bold line represents (a) $G_{\mathrm{EDP|IM}}(edp, im)$ and (b) $F_{\mathrm{IM}_{cap}|\mathrm{EDP}}(im', edp)$.

IM's and their associated IDA curves, together with their principal fractiles. Fixing an EDP level, PDF's and CDF's of IM_{cap} can be shown and compared to choose which investigated IM has the best influence on $G_{\mathrm{EDP|IM}}$. Fig. 2 shows that the IM in (a) is worse than that in (b), considering an EDP level equal to 0.3, and applied an IDA curve set of 40 recorded ground motions. It should be particularly noted the variation of the dispersion between the two proposals. Observing dispersion index is the best tool to compare different IM's with possible different units. So, we expect that the effect of a good IM reduces the dispersion level of the distribution of IM_{cap} associated at different ductility level, with the correspondent reduction of the uncertainty level associated to $\lambda_{\mathrm{EDP}}(edp)$ assessment.

Other two desirable IM properties are the *sufficiency* and the *scaling robustness*. The first characteristic concerns the statistical independence of conditional probability distribution of EDP given IM by other parameters used to calculate the seismic hazard at the site, like epsilon, ε, the earthquake magnitude, or the source-to-site distance. The last desirable property is for the structural response to be unbiased after the scaling operation to a value of IM (i.e., if it is compared to the analogous responses obtained from un-scaled ground motions). If a selected IM is "robust with scaling", then the structural response for scaled earthquake records do not show any bias towards their scale factors. This characteristic has an important role in PSDA, where scaled records are used to predict the probability of exceeding each value of EDP given the value of

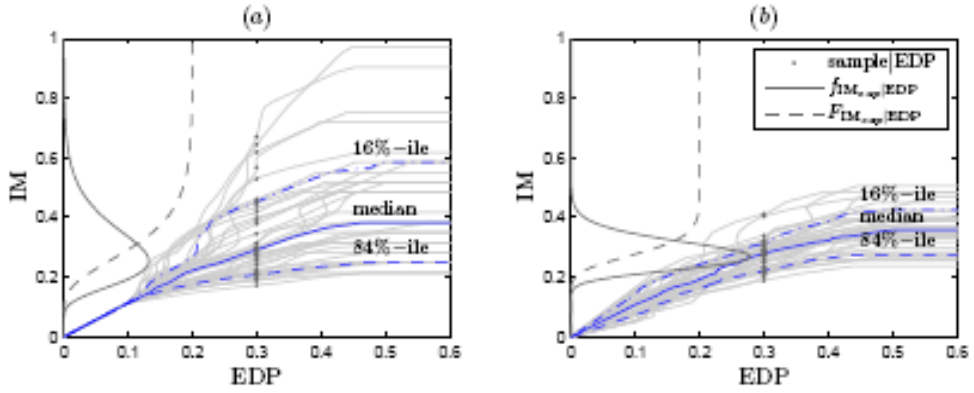

Figure 2: IDA curves and their principal fractiles for two different IM's, considering a set of 40 recorded ground motions. Comparison between (a) a bad IM and (b) a good IM, from an efficiency point of view.

the IM through IDA process. The study about $S_{a,avg}$ as IM in PBEE framework can be found in [11].

COMPUTATION OF $S_{a,avg}$

The description "average" of spectral accelerations can be interpreted in several ways, but in this work, we use this term to refer the geometric mean of the spectral pseudo-acceleration ordinates at 5% of damping:

$$S_{a,avg}(T_1,\ldots,T_n) = \left(\prod_{i=1}^{n} S_a(T_i)\right)^{1/n} \tag{3}$$

where $T_1,\ldots,T_n$ are the n periods of interest. In the light of the EDP-based rule, $S_{a,avg}$ becomes the proposed IM_{cap}. It should be noted that T_i does not mean the i-th natural period of vibration, but only the i-th value in the $(T_1,\ldots,T_n)$ set of periods. By taking logarithms of both sides of Equation (3), we can also express the geometric mean in the following form:

$$\ln S_{a,avg}(T_1,\ldots,T_n) = \frac{1}{n}\sum_{i=1}^{n} \ln S_a(T_i). \tag{4}$$

Equation (4) simply computes the arithmetic mean of the logarithm of spectral accelerations. It is more convenient because attenuation laws quote the results of regression analyses in terms of natural logarithm of spectral accelerations. Thus, an attenuation

law can be easily developed for $\ln S_{a,avg}$ with an arbitrary set of periods $T_1, \ldots, T_n$ using existing attenuation models (e.g., [1]). If a general attenuation law describes the ground motion intensity measure as a function of magnitude, distance and site geology in terms of natural period of vibration, then it can be proved that the regression coefficients for $\ln S_{a,avg}(T_1, \ldots, T_n)$ can be obtained simply by the mean of the regression coefficients for each $\ln S_a(T_i)$. Thus, PSHA can be performed using $\ln S_{a,avg}$ as intensity measure in the same way of any single spectral acceleration value. For example, in [15], three hazard analyses were performed for the Van Nuys site, using the Abrahamson and Silva [1] ground motion prediction model for the prediction of average of spectral accelerations at two selected periods.

Given that multiple $\ln S_a(T_i)$ values are jointly Gaussian distributed (or similarly that $S_a(T_i)$ values are jointly log-normally distributed) as is shown in [23], then a sum of them is Gaussian, and is fully described by the following expression of mean and variance:

$$\mu_{\ln S_{a,avg}} = \frac{1}{n} \sum_{i=1}^{n} \mu_{\ln S_a(T_i)}, \tag{5}$$

$$\sigma^2_{\ln S_{a,avg}} = \frac{1}{n^2} \sum_{i=1}^{n} \sum_{j=1}^{n} \rho_{\ln S_a(T_i), \ln S_a(T_j)} \sigma_{\ln S_a(T_i)} \sigma_{\ln S_a(T_j)}, \tag{6}$$

where $\mu_{\ln S_a(T_i)}$ and $\sigma_{\ln S_a(T_i)}$ are, respectively, the conditional mean and the standard deviation of $\ln S_a(T_i)$, available from popular ground motion attenuation models. It should be noted that the term *conditional* refers to the values for a given earthquake moment magnitude, site-to-source distance, site classification, etc.

The term $\rho_{\ln S_a(T_i), \ln S_a(T_j)}$ in Equation (6) represents the correlation between the spectral shape of a single horizontal ground motion component at two different periods T_i and T_j. This correlation can be written as [4]

$$\rho_{\ln S_a(T_i), \ln S_a(T_j)} = 1 - \cos\left[\frac{\pi}{2} - \left(0.359 + 0.163\, I_{(T_{min}<0.189)} \ln \frac{T_{min}}{0.189}\right) \ln \frac{T_{max}}{T_{min}}\right], \tag{7}$$

where T_{min} and T_{max} are, respectively, the smaller and the larger of T_i and T_j, and $I_{(T_{min}<0.189)}$ is an indicator function equal to 1 if $T_{min} < 0.189$ sec and equal to 0 otherwise.

The numerical value of $S_{a,avg}$ is affected by the selected number of periods n, and the corresponding spectral acceleration values $S_a(T_i)$, $i = 1, \ldots, n$, used to calculate the geometric mean. Hence, of particular interest is the case where one needs to compute spectral acceleration averaged over a period range from T_1 (i.e., the lower bound in the selected range) to T_n (i.e., the upper bound), and choose how many intermediate points to include. It could conceivably be true that if the generic suite of n period $(T_1, \ldots, T_n)$ is taken in the range of long periods (where the spectrum is more smooth), the necessary number of points will not play a leading role. On the contrary, in the range of short periods (where the variability of the spectrum is significative), different number of points will produce different results in terms of $S_{a,avg}$. Furthermore, the mathematical-spacing rule of the n periods will follow the same period-base trend presented above. So, in the long-period range an arithmetical- or logarithmic-spacing should not make a difference, whereas in the short-period range could affect in a relevant way the result. The potential difference lies in the sampled number of points by two mathematical-spacing: in fact, fixed a threshold values, arithmetic- generates less points than logarithmic-spacing. Although, defining uniquely what is the *exact* value of $S_{a,avg}$ is important, in this section we are not able to decide the necessary number of points and the mathematical-spacing rule of sampling. However, in order to continue with the logical path of the paper, we anticipate that $S_{a,avg}$ will be computed using ten points whatever spaced, and an explanation will be provided later.

SIMULATED SYSTEMS AND EARTHQUAKE RECORDS

A set of single- (SDOF) and multi-degree-of-freedom (MDOF) systems are considered in this study adopting an hysteretic nonlinear model that includes strength and stiffness deterioration properties [26]. The bilinear and peak oriented hysteretic model, which are normally used in seismic demand analysis, are adopted here, respectively, for SDOF and MDOF systems, as shown in Fig. 3. They integrate an energy-based deterioration parameter, $\gamma_{s,c,k,a}$, that controls the cyclic deterioration modes (basic strength, post-capping strength, unloading stiffness, and accelerated reloading stiffness deterioration). The backbone curve without deterioration property is totally defined by the elastic initial stiffness, K_e, the yield strength, F_y, and the strain-hardening stiffness, $K_s = \alpha_s K_e$, where α_s represents the strain hardening. If deterioration is included, the backbone

curve is completed by the ductility capacity (i.e., the ratio between the displacement at the peak strength, δ_c, and the yield displacement δ_y) and the post-capping stiffness ratio, α_c, which controls the softening branch such that the post-capping stiffness can be written as $K_c = \alpha_c K_e$. In addition, a residual strength, F_r, can be introduced in the model to ensure a lower threshold when cyclic deterioration shrinks the backbone curve. Both for SDOF and MDOF systems, the critical damping is assumed to 5% value in accord with the viscous damping allowed in FEMA 356 [**?**]. A detailed description of backbone curve and hysteretic models can be found in [21]. The resulting structural demand parameter considered in this paper is the maximum peak inter-storey drift angle, θ_{max}.

Thought the previous models are calibrated to describe the behavior of a component, we assume that the response of SDOF systems follows the same hysteresis and deterioration rules as a representative component. This is a simplifying assumption, as it is idealistic to assume that all components of structural system have the same deterioration properties and yield and deteriorate simultaneously. Anyway, this assumption is acceptable when buildings are dominated by elastic first-mode, i.e., when they can assumed a SDOF systems. In order to display the influence of deterioration property of the bilinear model in structural response, two sets of SDOF systems with the same strain hardening ratio ($\alpha_s = 5\%$) are considered here: the first one is characterized by $\delta_c/\delta_y \to \infty$, hence α_c becomes unessential, whereas the second one has $\delta_c/\delta_y = 4$ and $\alpha_c = -25\%$. Neither cyclic deterioration effects ($\gamma_{s,c,k,a} \to \infty$), nor residual strength ($F_r = 0$) are considered in our examples of real structures dominated by elastic first-mode. Each set is composed by five systems with different periods, such that $T^{(1)} = 0.3, 0.6, 1.0, 1.5$ and 3.0 sec; we do not specify δ_y because, assuming the EDP-based rule (i.e., given an EDP value), the result are unrelated to this parameter.

The first set of MDOF systems considered in this work is constituted by two-dimensional regular generic frames of a single bay and several stories, modeled and analyzed in [21]. Twelve moment-resisting frames, that cover the range of low- and mid-rise structure and with a variety of structural properties, represent this set of MDOF systems. They have six different number of stories, $N = 3, 6, 9, 12, 15$ and 18, and the fundamental period of the structure is associated with this number. We identify MDOF systems whit fundamental period $T^{(1)} = 0.1N$ as "stiff moment-resisting frames", and

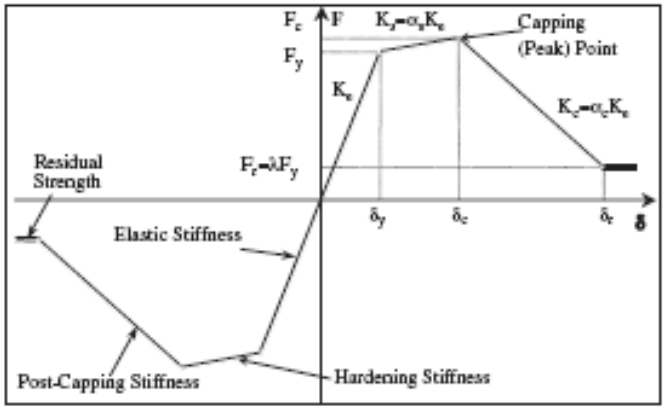

Figure 3: Backbone curve for hysteretic models of Ibarra-Medina-Krawinkler.

with "flexible moment-resisting frames" when $T^{(1)} = 0.2N$. The peak-oriented hysteretic model, which is considered at the beam ends and at the base columns, is used for all the structures. It utilizes $\gamma_{s,c,k,a} \to \infty$, as well as the following backbone curve parameters: $\alpha_s = 3\%$, $\delta_c/\delta_y = 4$, $\alpha_c = -10\%$, and $F_r = 0$. Each structure has a single bay with story stiffness and strengths chosen to be representative of typical structures. Global P-Δ effects are included, whereas member P-δ are disregarded, as well as axial deformations and P-M-V interaction. Especially when the height of the floor is noticeably high (say greater than 9), these MDOF systems are particularly influenced to higher-mode excitations, because relative element stiffness are designed to obtain a straight line deflected shape for the first mode, and columns in a story and beams above them have the same moment of inertia. In accord with [20], where these MDOF systems are presented and exhaustively described, here we identify them as *reference frames*.

In order to work as well with more realistic structures, we choose a second set of MDOF systems based on the same peak-oriented hysteretic model presented above. Unlike reference frames, where beams and columns undergo both shear and flexural deformations, in this second set of structures the ratio of span and depth of elements is designed so that shear deformations in individual members are small than the flexural contributions, i.e., the lateral deformation is poorly affected by shear-type behavior. Eight moment-resisting frames with number of stories equal to $N = 4, 8, 12$ and 16 are here considered. Similarly to reference frames, they are subdivided in "stiff" and "flexible" frames, because the fundamental period of the structure is, respectively, $T^{(1)} =$

$0.1N$ and $T^{(1)} = 0.2N$. These MDOF systems are deeply described in [38], and they are identified here as *supporting frames*.

Both SDOF and MDOF systems are subjected at the same set of 40 ordinary ground motions recorded in California, and they are chosen as significant statistical sample of time histories. These records were used in [20] and [38]. They do not exhibit pulse-type near-fault characteristics and are recorded on stiff soil or soft rock, corresponding to soil type D according to FEMA 356 [**?**]. The source-to-site distance, R_{rup}, ranges from 13 to 40 km and the moment magnitude, M_w, from 6.5 to 6.9. Additional characteristics requested for this set of 40 ordinary ground motions are briefly summarized: (i) strike-slip, reverse-slip and reverse-oblique fault mechanisms are considered; (ii) for each station, one horizontal component is randomly selected; (iii) aftershocks are not included; (iv) the high-pass corner frequency is less or equal than 0.20 Hz. This requirement influences noticeably the recorded time history and the shape of the elastic and inelastic spectra, especially when oscillator periods are much shorter than the reciprocal of the high-pass corner. This undesirable effect has been shown for severe levels of inelastic response and it due to the effective period lengthening that occurs when oscillator behave inelastically [10]. The use of a single set of GMs is acceptable because it has been shown that inelastic response of systems is not greatly affected by M_w and R_{rup} (except for near-fault regions). Regarding the size of the set of GMs, the uncertainty associated with the estimated EDPs and collapse capacities may be quantified as a function of the number of data points evaluated in the form of confidence levels. The use of a set of 40 GMs provides estimates of the median that are within a one-sigma confidence band of 10% as long as the standard deviation of the natural logarithm of the collapse capacities or EDPs is less than $0.1\sqrt{40} = 0.63$.

RESPONSE PREDICTION USING $S_{a,avg}$

As previously mentioned, in order to obtain a reliable assessment of response prediction in PBEE framework, a "good" IM must hold some desirable properties, such as efficiency, sufficiency, scaling robustness and hazard-computability. This study focuses on the efficiency property of $S_{a,avg}$ as IM, i.e., evaluating $\sigma_{\ln(S_{a,avg}|\mathrm{EDP})}$. We remind that at random variable EDP can be associated with a ductility level μ. We calculate $S_{a,avg}$ using ten points arithmetic and logarithmic spaced in the interval $(T_1, \ldots, T_n)$.

Furthermore, we suppose that T_1 and T_n are unknown, but we want to tie both of them to the fundamental period of the structure, $T^{(1)}$. So, the average of spectral accelerations is calculated with ten points whatever spaced in the interval such that $T_1 = k_l\, T^{(1)}$, and $T_n = k_u T^{(1)}$, where k_l and k_u are constants specifying lower and upper period bounds, respectively, relative to $T^{(1)}$. The constant k_l is chosen to vary between $T_{low}/T^{(1)}$ and 1, whereas k_u between 1 and $T_{upp}/T^{(1)}$, where T_{low} and T_{upp} are, respectively, the lower and the upper period of the elastic spectrum (which is constrained by the filter frequencies of the ground motions). When $k_l = k_u = 1$, we simply obtain $S_{a,avg}(T^{(1)}, \ldots, T^{(1)}) = S_a(T^{(1)})$.

For MDOF systems, the lower bound $k_l T^{(1)}$ captures the higher-mode influence on the dynamic behavior of systems, while the upper one $k_u T^{(1)}$ the response when the structure is damaged, and its effective period is lengthened. For SDOF systems, which have one natural period of vibration, it does not make sense to speak of higher-mode contributions. So, the interval where $S_{a,avg}$ is calculated becomes simply $(T^{(1)}, \ldots, k_u\, T^{(1)})$. Furthermore, if the system (whatever with single- or multi- degree-of-freedom) is modeled with an elastic behavior, then $k_u \geq 1$ does not make sense, because the range from $T^{(1)}$ onwards is the interval where the damaged structure inelastically modeled has its dynamic behavior.

Tendency for single-degree-of-freedom systems

When the structure is first-mode dominated, it is often acceptable consider it as a SDOF system, and the interval ranges between $T^{(1)}$ and $k_u\, T^{(1)}$. For any increment of k_u, between 1 and $T_{upp}/T^{(1)}$ the dispersion is calculated. This procedure was repeated for all SDOF systems (with and without post-capping value) and for μ ranges between 1 to 6. The results can be displayed in a diagram which shows k_u versus $\sigma_{\ln(S_{a,avg}|\mathrm{EDP})}$, where we assign that *edp* level associated with a ductility level μ: we identify this graphic trend as *k-sigma curve*. As example, Fig. 4 shows the k-sigma curve for the SDOF system with fundamental period $T^{(1)} = 1$ sec, $\alpha_c = -25\%$, and $\delta_c/\delta_y = 4$, chosen as representative of all SDOF systems. In particular, Fig. 4 shows the dispersion assuming (a) arithmetic- and (b) logarithmic-spacing, using ten points between $T^{(1)}$ and $k_u\, T^{(1)}$. For $\mu \leq 4$ there are no differences in results vetween the two structures, because until $\mu = 4$ the SDOF systems have the same dynamic behavior. Anyway, the differences

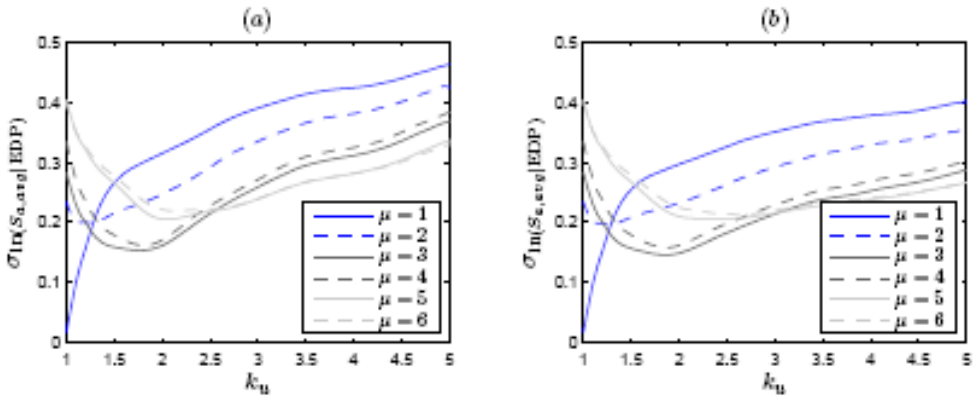

Figure 4: k-sigma curve of $S_{a,avg}(T^{(1)}, \ldots, k_u T^{(1)})$ for SDOF system (deterioration parameter included) with $T^{(1)} = 1$ sec and $\delta_c/\delta_y = 4$, differentiated for (a) arithmetic- and (b) logarithmic-spacing rule using ten points between $T^{(1)}$ and $k_u\, T^{(1)}$. The given ductility level, μ, ranges between 1 and 6.

between systems with backbone curve elastic-plastic and elastic-plastic-degradation are not significant.

For all SDOF systems, in the elastic ($\mu = 1$), or almost-elastic ($\mu = 2$), case, the minimum of the dispersion occurs when k_u is approximately equal to 1, meaning that S_a is the best predictor. However, for $\mu \geq 2$, $S_{a,avg}$ becomes significantly better than S_a, but the minimum level of dispersion is reached at different k_u level, that we call *optimal value*, $k_{u,opt}$. To better visualize this trend, Fig. 5 shows a simple linear regression analysis between $k_{u,opt}$ and $\sigma_{\ln(S_{a,avg}|\mathrm{EDP})}$. This fitting curve, identified by $\hat{k}_u$, proves that when μ increases also k_u increases, and this relation can be strongly linear, even if slope and absolute value change with $T^{(1)}$. Alternatively, Fig. 5 shows also $\bar{k}_u$, which simply averages the $k_{u,opt}$. As usual, the chart is differentiated between (a) arithmetic- and (b) logarithmic-spacing rule. The difference between the two spacing method is lesser than the 10% for all the considered SDOF systems, whatever with or without deterioration parameter. In order to check the goodness of the linear approximation (both of sloping and horizontal), also we plot the 10% of deviation from the minimum of the dispersion. For any μ, $\hat{k}_u$ falls within the simulated 10%-error, whereas $\bar{k}_u$ is sometimes wrong, especially for the bound of ductility interval. Arithmetic- and logarithmic-spacing provide the same minimum level of dispersion, but a slight difference in terms of the best k_u coefficient. For the arithmetic- and logarithmic-spacing, the optimal coefficient, $k_{u,opt}$,

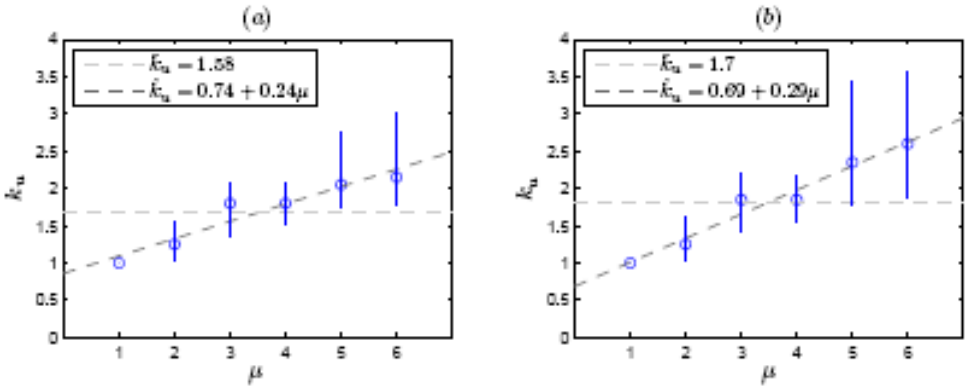

Figure 5: Linear regression analysis, $\hat{k}_u$, between the minimum of the sigma-curves and μ, together with the averaged minimum value, $\bar{k}_u$, differentiated for (a) arithmetic- and (b) logarithmic-spacing rule using ten points between $T^{(1)}$ and $k_u\,T^{(1)}$, for SDOF system (deterioration parameter included) with $T^{(1)} = 1$ sec and $\delta_c/\delta_y = 4$. The vertical stripes represents the 10% of deviation from the minimum of the dispersion.

ranges, respectively, from 1.50 to 2.35, and from 1.60 to 2.70. The mean values in terms of spacing rules are, respectively, 1.80 and 2.00. This variability depends on the period of the SDOF system, and k_u increase when $T^{(1)}$ decreases. Results for arithmetic- are less scattered than the logarithmic-spacing, but k-sigma curves for the second rule are more flat than the first one: considering a little error between $k_{u,opt}$ and the assumed value, $k_{u,ass}$, logarithmic-spacing shows a better adequacy for all level of given ductility level. However, we are not still able to state which mathematical-spacing rule is the best, because this validation is quite weak. If we focus the attention between structures with or without deterioration parameter, $k_{u,opt}$ ranges between similar bounds (from 1.5 to 2.70, with a mean value equal to 1.90) and data are equally scattered, confirming there are no differences between the two systems.

Tendency for multi-degree-of-freedom systems

When the dynamic behavior of structures is sensitive to higher-mode periods, it is necessary to include also a variable lower bound, $T_1 = k_l T^{(1)}$, in addition to the upper one, $T_n = k_u T^{(1)}$, to evaluate which range of periods is better to use to calculate $S_{a,avg}$.

At the beginning we choose to assign k_u value and observing the trend of $\sigma_{\ln(S_{a,avg}|\mathrm{EDP})}$ in k-sigma curve of MDOF systems when k_l varies between $T_{low}/T^{(1)}$ and 1. As example,

Fig. 6 and Fig. 7 shows the shape of k-sigma curve for a MDOF system with $T^{(1)} = 1.2$ sec and $N = 12$ floors, and $\delta_c/\delta_y = 4$, using ten points, respectively, arithmetical and logarithmic spaced between $k_l T^{(1)}$ and $k_u T^{(1)}$. In particular, we assign k_u equal to (a) 1.5, (b) 2.0, and (c) 2.5. These values are not random numbers, but we chose them so that there is a link with the results obtained for SDOF systems. In fact, we obtained that $k_{u,opt}$ is about 2.0, and here we use a discrete range centered in $k_{u,opt}$. The biggest difference is that the results obtained with arithmetical spacing (Fig. 6) seem to be quite indifferent to interval width in terms of k_l, especially in the inelastic case: in fact, when $\mu \geq 3$, the curves tend to become flat. This insensitivity to k_l at any ductility levels is more marked when k_u increases, even if $\sigma_{\ln(S_{a,avg}|\mathrm{EDP})}$ still increases. This flat-trend to k_l coefficient could be a good goal, if the dispersion does not raise. Anyway, it should be noted that for small value k_u, the dispersion obtained using a large range in lower band is relevantly different to that using a short range. At the opposite, when k_u is small, the choice in terms of k_l. For a assigned value of k_u, logarithmic-spacing rule (Fig. 7) seems better than arithmetic- one, because it can be found a confined range of k_l values where the dispersion preserve its minimum value. This range of period is not constant for all MDOF systems, but it can be identified by $T^{(1)}$ for all the systems. Finally, the comparison between Fig. 6 and Fig. 7 leads us to choose logarithmic spacing as better sample rule of intermediate period between T_1 and T_n to calculate $S_{a,avg}$.

Without assigning a particular value of k_u, now we calculate $\sigma_{\ln(S_{a,avg})|\mathrm{EDP}}$ varying k_l from $T_{low}/T^{(1)}$ to 1, and k_u from 1 to $T_{upp}/T^{(1)}$. Since we have two variables, the k-sigma curve becomes reasonably a *k-sigma surface*, which will be better visualized by its contour plot. As previously mentioned, the range of k_u values which minimizes the dispersion depends on the particular structure. In fact, it is conceivable thinking that for the structures dominated by the first-mode, $k_{l,opt}$ ranges in the values around 1, because essentially higher-mode influence does not relevantly affect the dynamic behavior of the MDOF system. Hence, these structures can be studied as SDOF systems, and the effective interval where $S_{a,avg}$ is calculated become simply $(T^{(1)}, \ldots, k_u\, T^{(1)})$. As example, Fig. 8 and Fig. 9 show the contour of k-sigma surface of $S_{a,avg}$ with ten points logarithmical-spaced for MDOF systems (respectively, reference and supporting frames) with fundamental period in the short, medium and large range of the spectrum, and for selected given ductility level. We chose to show the k-surface only for $\mu = 2, 4, 6$ as

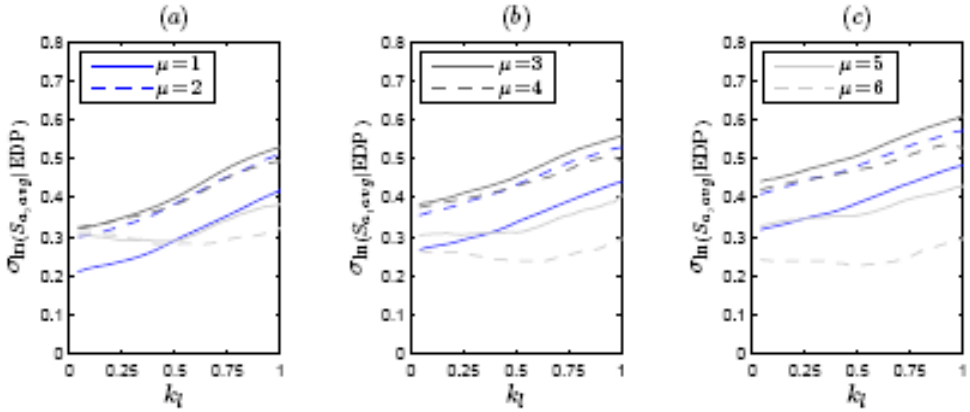

Figure 6: k-sigma curve of $S_{a,avg}(k_l\,T^{(1)},\ldots,k_u\,T^{(1)})$ assuming ten points arithmetical spaced, for MDOF system (reference frames) with $T^{(1)}=1.2$ sec, $N=12$ floors, and $\delta_c/\delta_y=4$, assigning (a) $k_u=1.5$, (b) $k_u=2.0$, and (c) $k_u=2.5$. The given ductility level, μ, ranges between 1 and 6.

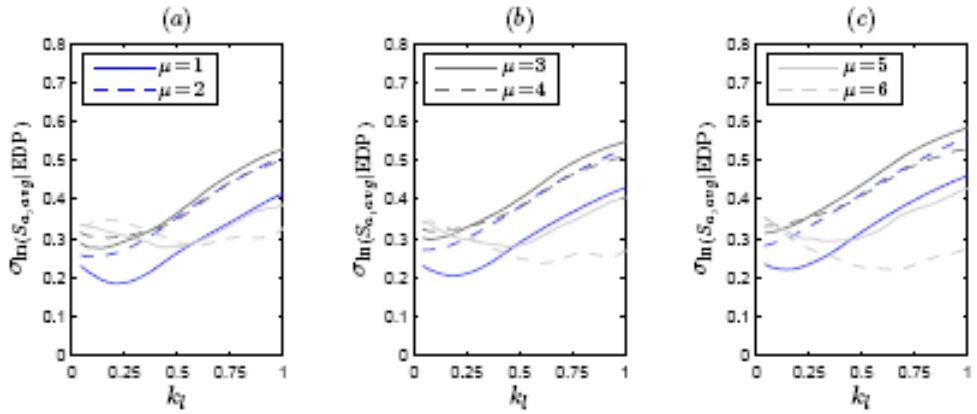

Figure 7: k-sigma curve of $S_{a,avg}(k_l\,T^{(1)},\ldots,k_u\,T^{(1)})$ assuming ten points logarithmical spaced, for MDOF system (reference frames) with $T^{(1)}=1.2$ sec, $N=12$ floors, and $\delta_c/\delta_y=4$, assigning (a) $k_u=1.5$, (b) $k_u=2.0$, and (c) $k_u=2.5$. The given ductility level, μ, ranges between 1 and 6.

representative value of ductility level lesser than the selected one: as it can be deduced from Fig. 4 for SDOF or Fig. 7 for MDOF systems, similar trend are obtained for $\mu = 1, 3, 5$. In this way, we can visualize how k_l becomes small for those MDOF systems which are affected by higher-mode influence, whereas tends to 1 for those structure which are first-mode dominated. Hence, we can conclude that the optimal coefficient for the lower bound, $k_{l,opt}$ is around equal to 0.25 for the MDOF systems affected by higher-mode influence; otherwise, k_l can be set equal to 1 without making big mistakes. At the opposite, k_u becomes relevant for MDOF systems dominated by the first mode and the value matches the value found for SDOF systems, i.e., $k_{u,opt} \approx 2$. This is particularly true for small and medium ductility level, but $k_{u,opt} \approx 3$ should be taken for $\mu \geq 4$. This conclusion is consistent with the trend of SDOF systems. Otherwise, i.e., for structures with medium-long periods, k_u can be assigned to 1.

About number of points

We revisit here the question of how many periods, n, are needed in the interval $(T_1, \ldots, T_n)$ to calculate $S_{a,avg}$. We could define the true value of an average of spectral accelerations as that value obtained by Equation (3), or (4), using n equal to one hundred points, $S^{100}_{a,avg}$, logarithmically spaced. Nevertheless, $S^{100}_{a,avg}$ is used here just as element of comparison between different choices in terms of n. We anticipate that one hundred points are not needed, because the difference is small, even for n values much less than 100.

We consider the SDOF systems and n points between $(T^{(1)}, \ldots, k_u T^{(1)})$, and by varying k_u from 1 to $T_{upp}/T^{(1)}$. As previously done, for a fixed value of coefficient k_u, $S_{a,avg}$ can be determined for any records through Equation (3) and the population can be described by the median and the dispersion of these outcomes, assuming that IM and EDP levels are lognormally distributed. For a fixed value of k_u, PDFs can be compared in terms of number of points. As an example, fixing a value of given ductility level, e.g., $\mu = 3$, and considering the SDOF system with $T^{(1)} = 1$ sec, it can be shown that $S_{a,avg}$ with ten points, Fig. 10(b), well approaches the result obtained using one hundred points, whereas the results obtained using only two points, shown in Fig. 10(a), are sometimes unacceptable. This matching is more clear watching the PDFs for different k_u values, set to 1.5, 2, 2.5 and 3, and ten points is the best solution for any interval

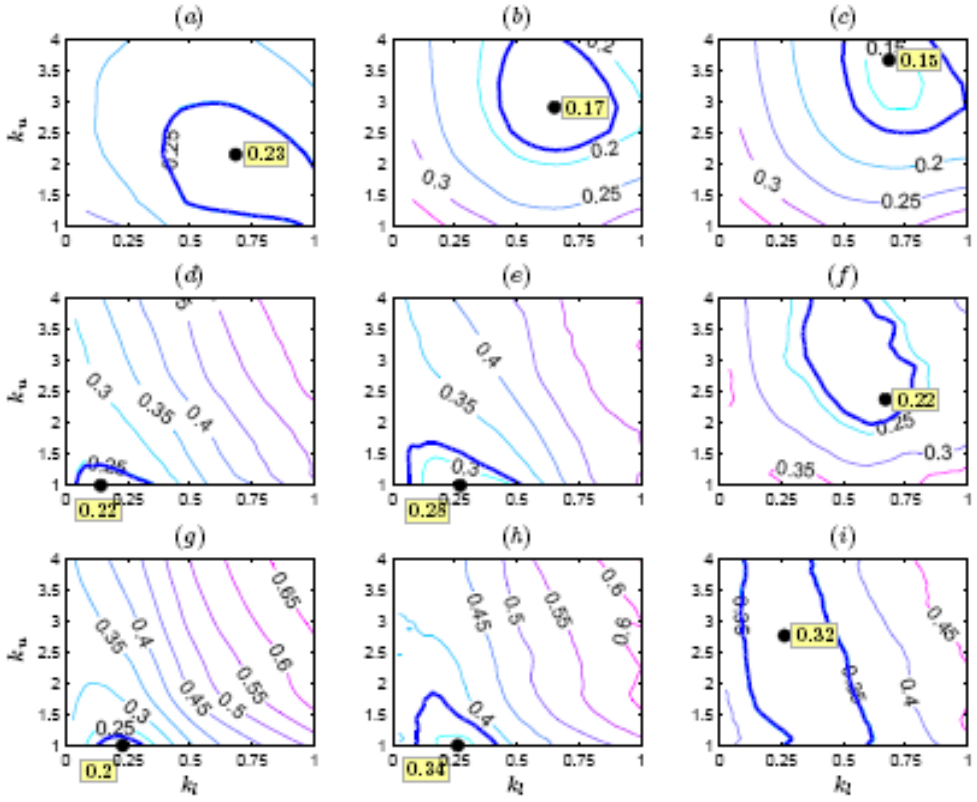

Figure 8: k-sigma contour plot of $S_{a,avg}(k_l T^{(1)}, \ldots, k_u T^{(1)})$ assuming the logarithmic-spacing rule, for MDOF systems (reference frame) with $\delta_c/\delta_y = 4$ and (a, b, c) $T^{(1)} = 0.6$ sec and $N = 6$ floors, (c, d, e) $T^{(1)} = 1.2$ sec and $N = 12$ floors, and (f, g, h) $T^{(1)} = 1.8$ sec and $N = 18$ floors. The selected given ductility levels, μ, are chosen in 2, 4 and 6 (from left to right. The bold line represents the 10% of deviation from the minimum of the dispersion.

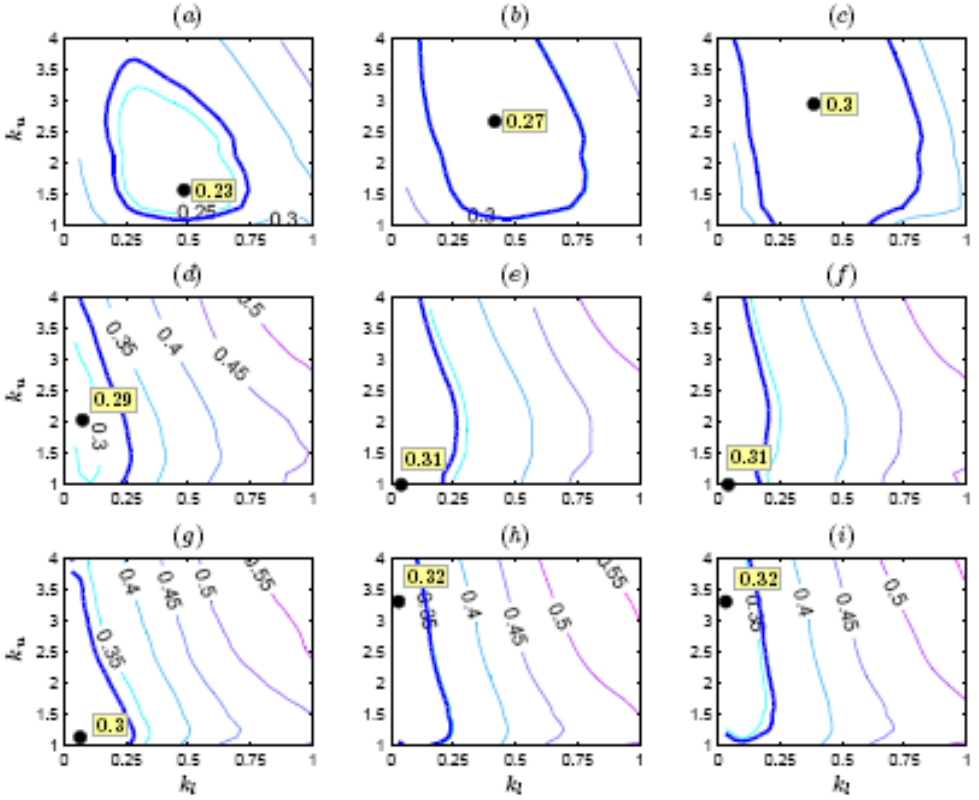

Figure 9: k-sigma contour plot of $S_{a,avg}(k_l T^{(1)}, \ldots, k_u T^{(1)})$ assuming the logarithmic-spacing rule, for MDOF systems (supporting frame) with $\delta_c/\delta_y = 4$ and (a, b, c) $T^{(1)} = 0.8$ sec and $N = 8$ floors, (c, d, e) $T^{(1)} = 1.2$ sec and $N = 12$ floors, and (f, g, h) $T^{(1)} = 1.6$ sec and $N = 16$ floors. The selected given ductility levels, μ, are chosen in 2, 4 and 6 (from left to right). The bold line represents the 10% of deviation from the minimum of the dispersion.

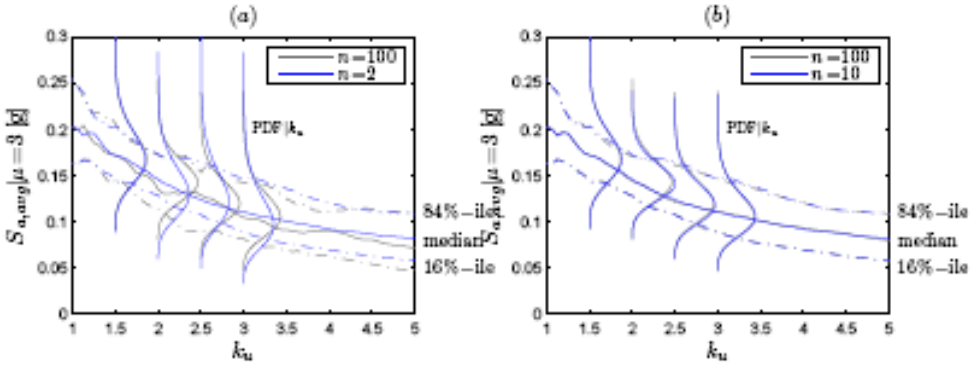

Figure 10: Influence of the number of points used to calculate the average in the interval $(T_1, \ldots, T_n)$, where $T_n = k_u T^{(1)}$, on the 16%, 84% and median of $S_{a,avg}$ versus the coefficient k_u for SDOF system (deterioration parameter included) with $T^{(1)} = 1$ sec, $\delta_c/\delta_y = 4$, and for $\mu = 3$: comparison between logarithmic-spacing rule with (a) $n = 2$ and (b) $n = 10$, always assuming $n = 100$ as a reference level. PDFs are shown at several ductility levels.

width. The mathematical-spacing rule does not affect in a relevant way the results.

The same trend was observed in all SDOF systems and at all given ductility levels, and results were obtained for MDOF systems. It is also expected that these conclusions can be extended to different bins of earthquake time histories, as specific records properties do not affect the results considered here. Based on these results, it is recommended that 10 periods be used when calculating $S_{a,avg}$. However, it should be noted that numerical results state a decrease of the accuracy of this assessment for small value of $T^{(1)}$ together with a huge interval. Basically, it could be disregarded because $S_{a,avg}$ is always computed in a midsize band of periods.

DISCUSSION

In this section we present the results obtained by comparison of different IMs, elastic and inelastic, with $S_{a,avg}$ calculated in the light of previous considerations. We focus the attention on the first integrand in Equation (2), and in particular we analyze the efficiency of the selected IMs. In other words, we compare the dispersion of IM given a certain level of EDP. Ductility levels between 1 and 6 were considered, in order to observe the effectiveness of the IM's for linear response up to significantly nonlinear response.

Fig. 11-*a* shows the trend of different IMs for deteriorating SDOF system with $T^{(1)} = 1.0$ sec. Here, $S_{a,avg}$ shows the best efficiency compared with other IMs. Peak ground parameters seems to follow a relation between the kinematic-sensitive region in the elastic spectrum and the fundamental period of the structures. In this way, PGA show a good level of efficiency for structure dominated by the first mode, sometimes better than $S_a(T^{(1)})$, whereas PGD is better for long period. $S_{a,avg}$ show for any SDOF systems (with or without deterioration parameter) the best level of dispersion, except for S_{di}. It should be noted that for SDOF systems without deterioration parameter, the level of dispersion is exactly zero, because EDP matches exactly the inelastic spectral displacement. Similar trend can be found for the MDOF systems, showed in Fig. 11-*b*, -*c*,-*d*, respectively, for the short, medium and long fundamental period. However, with MDOF systems the link between peak ground parameters and kinematic sensitivity region is partially lost, and sometime it's the opposite of the SDOF trend. The inelastic spectral displacement is more efficient than the elastic spectral acceleration for short fundamental period, and becomes comparable for medium and long $T^{(1)}$. On the contrary, $S_{a,avg}$ preserves its low dispersion for any given ductility level and for any fundamental period.

CONCLUSIONS

In this work, a new IM based on a geometric mean of n spectral accelerations at 5% of damping, namely $S_{a,avg}\,(T_1, \ldots, T_n)$, or simply $S_{a,avg}$, has been proposed as an effective predictor of inelastic structural response. The demand assessment via probabilistic perspective represents a core point in PSDA. In general, the complementary cumulative distribution function (CDF) of EDP given an IM level, $G_{\mathrm{EDP|IM}}\,(edp, im)$, is jointly integrated to the MAF of exceeding a certain level of IM at the site to produce a MAF of exceeding an EDP level, $\lambda_{\mathrm{EDP}}\,(edp)$. It is preferable to express the link between ground motion hazard parameter and structural response through the CDF of IM capacity given a certain ductility level, $F_{\mathrm{IM}_{cap}}\,(im, edp)$. Anyway, it is still possible to determine $\lambda_{\mathrm{EDP}}\,(edp)$ through $F_{\mathrm{IM}_{cap}}\,(im, edp)$ as well as $G_{\mathrm{EDP|IM}}\,(edp, im)$, and it has been shown this similarity. Some considerations has been done also about the easy computation of PSHA in terms of $S_{a,avg}$ compared to inelastic and vector-valued IMs. In fact, the necessity to couple an hazard curve at the site-easily assessable to low levels

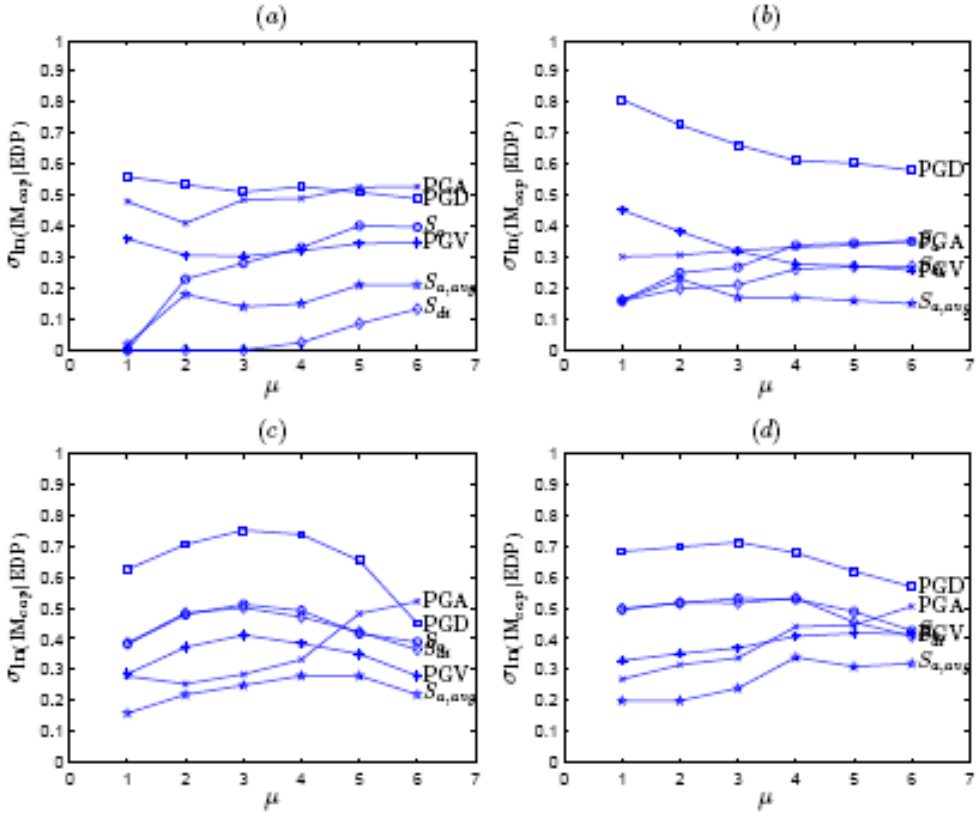

Figure 11: Comparison between different IMs in terms of $\sigma_{\ln(IM)|EDP}$ for (a) SDOF system (deterioration parameter inclueded) with $T^{(1)} = 1.0$ sec, and MDOF systems (reference frames) with (b) $T^{(1)}=0.6$ sec and $N=6$ floors, (c) $T^{(1)}=1.2$ sec and $N=12$ floors, (d) $T^{(1)}=1.8$ sec and $N=18$ floors.

of dispersion represents the main task that lead us in finding a new IM.

The choice of $F_{\mathrm{IM}_{cap}}(im, edp)$ is consistent with the EDP-based rule applied to IDA curve set, and it has the advantage to carry out statistical evaluation unaffected by outliers in terms of dispersion at different EDP levels. In fact, the goal of this work has been to show the effciency of $S_{a,avg}$ compared to traditional elastic, e.g., the elastic pseudo.spectral acceleration at the fundamental period of structure, $S_a\left(T^{(1)}\right)$, or peak-ground parameters, and advanced IM, e.g., the inelastic spectral displacement, S_{di}. To more clearness, the effciency property of an IM concerns the dispersion of IDA curve set given an EDP or IM level, in terms of the natural logarithm of standard deviation of the sample. Furthermore, increasing the effciency property of an IM, the number of necessary time histories to employ in PSDA decreases.

In order to compare the effectiveness of $S_{a,avg}$ with other IMs, a set of inelastic SDOF and MDOF systems was chosen as representative of dynamic behavior of different types of buildings. Furthermore, 40 ordinary ground motions were selected as a representative sample of time histories. A hysteretic bilinear model with and without deterioration parameter identify two subsets of SDOF systems, to display the infuence of softening branch on the effciency of IMs. A peak-oriented hysteretic model has been applied to two different classes of MDOF system, differentiated by the presence of higher-mode effects.

The study has presumed the complete ignorance about the mathematical-spacing rule to catch n spectral ordinates, their number and the defnition of the interval $(T_1, \ldots, T_n)$. In reference to the last aspect, we has chosen to lie the range of periods where calculate $S_{a,avg}$ to the fundamental period of the considered structures, $T^{(1)}$, such that $T_1 = k_l T^{(1)}$ and $T_n = k_u T^{(1)}$, where k_l and k_u are, respectively, the lower and the upper bound coeffcient. In particular, $\left(T^{(1)}, \ldots, k_l T^{(1)}\right)$ has been used for SDOF systems, where higher-mode are clearly nonexistence, whereas $\left(k_u T^{(1)}, \ldots, k_l T^{(1)}\right)$ has been assumed for MDOF systems. k_u is relevant for SDOF systems, where it varies from 2.00 (low ductility level) to 3.00 (high ductility level). The last trend is still the same for MDOF systems dominated by the first mode, whereas k_u can be assumed equal 1 for MDOF systems with long period. Concerning the higher-mode effect, we can state that k_l oscillates around 0.25 for MDOF systems with higher-mode influence; otherwise, $k_l = 1$. Finally, using ten points logarithmically spaced to compute Sa;avg has resulted more

effcient than the same number of periods arithmetically spaced, because for the last method of sampling it is associated to particular insensitivity towards k_l, given a k_u level, but also a high level of dispersion.

BIBLIOGRAPHY

[1] Abrahamson N.A. and Silva W.J., 1997. Empirical response spectral attenuation for shallow crustal earthquakes. *Seismological Research Letters*, Vol. 68, No. 1, pp. 94-127.

[2] ASCE, 2005. *Minimum Design Loads for Buildings and Other Structures*, prepared by the American Society of Civil Engineers, Reston, VA.

[3] Baker J.W. and Cornell C.A., 2005. A vector-valued ground motion intensity measure consisting of spectral acceleration and epsilon. *Earthquake Engineering and Structural Dynamics*, Vol. 34, No. 10, pp. 1193-1217.

[4] Baker J.W. and Cornell C.A., 2006. Correlation of response spectral values for multicomponent ground motions. *Bulletin of the Seismological Society of America*, Vol. 96, No. 1, pp. 215-227.

[5] Baker J.W. and Cornell C.A., 2006. Spectral shape, epsilon and record selection. *Earthquake Engineering and Structural Dynamics*, Vol. 35, No. 9, pp. 1077-1095.

[6] Bazzurro P. and Cornell C.A., 1994. Seismic hazard analysis of nonlinear structures I: methodology. *Journal of Structural Engineering*, Vol. 120, No. 11, pp. 3320-3344.

[7] Bazzurro P. and Cornell C.A., 1994. Seismic hazard analysis of nonlinear structures II: applications. *Journal of Structural Engineering*, Vol. 120, No. 11, pp. 3345-3365.

[8] Bazzurro P. and Cornell C.A., 1999. Disaggregation of seismic hazard. *Bulletin of the Seismological Society of America*, Vol. 89, No. 2, pp. 501-520.

[9] Bazzurro P. and Cornell C.A., 2002. Vector-valued probabilistic seismic hazard analysis. *The Seventh U.S. National Conference on Earthquake Engineering*, hosted by the Earthquake Engineering Reserach Institute, Boston, MA.

[10] Bazzurro P., Sjoberg B., Luco N., Silva W. and Darragh R., 2004. Effects of strong motion processing procedures on time histories, elastic and inelastic spectra. *Workshop on Strong-Motion Record Processing (COSMOS)*, Richmond, CA.

[11] Bianchini M., Cornell C.A. and Baker J.W., 2008. An earthquake intensity measures based on an average of spectral accelerations. *Earthquake Engineering and Structural Dynamics* (in preparation).

[12] Benjamin J.R. and Cornell C.A., 1970. *Probability, statistics, and decision for civil engineers*. McGraw-Hill, New York, 684 pp.

[13] Bommer J.J., Magenes G., Hancock J. and Penazzo P., 2004. The influence of strong-motion duration on the seismic response of masonry structures. *Bulletin of Earthquake Engineering*, Vol. 2, No. 1, pp. 1-26.

[14] Chopra A.K., 2006. *Dynamics of structures: theory and applications to earthquake engineering*. Prentice Hall, New Jersey, 912 pp.

[15] Cordova P.P., Deierlein G.G., Mehanny S.S.F. and Cornell C.A., 2001. Development of a two-parameter seismis intensity measure and probabilistic assessment procedure. *Proceeding of the Second U.S.-Japan Workshop on PBEE Methodology for RC Building Structures*, Sapporo, Japan, pp. 195-214.

[16] Cornell C.A., 1968. Engineering seismic risk analysis. *Bulletin of the Seismological Society of America*, Vol. 58, No. 5, pp. 1583-1606.

[17] Cornell C.A., 1969. A probability-based structural code. *Journal of the American Concrete Institute*, Vol. 66, No. 12, pp.974-985.

[18] Cornell C.A., Fatemeh J., Hamburger R.O. and Foutch D.A., 2002. Probabilistic basis for 2000 SAC/FEMA steel moment frameguidelines. *Journal of Structural Engineering*, Vol. 128, No. 4, pp. 526-533.

[19] Cornell C.A. and Krawinkler H., 2000. Progress and challenges in seismic performance assessment. *PEER Center News*, Vol. 3, No. 2.

[20] Ibarra L.F. and Krawinkler H., 2005. Global collapse of frame structures under seismic excitations. *Report No. 152*, 2005. Department of Civil and Environmental Engineering, Stanford University, Stanford, CA.

[21] Ibarra L.F., Medina R.A. and Krawinkler H., 2005. Hysteretic models that incorporate strength and stiffness deterioration. *Earthquake Engineering and Structural Dynamics*, Vol. 34, No. 12, pp. 1489-1511.

[22] ICC, 2006. *International Existing Building Code*, prepared by the International Code Council.

[23] Jayaram N. and Baker J.W., 2008. Joint probability distributions of spectral acceleration values. *Bulletin of the Seismological Society of America* (in press).

[24] Luco N. and Cornell C.A., 2007. Structure-specific scalar intensity measures for near-source and ordinary earthquake ground motions. *Earthquake Spectra*, Vol. 23, No. 2, pp. 357-392.

[25] McGuire R.K., 2004. *Seismic hazard and risk analysis*. Ed. EERI, Berkeley, CA.

[26] Medina R.A. and Krawinkler K., 2003. Seismic demands for nondeteriorating frame structures and their dependence on ground motions. *Report No. 144*, 2003. Department of Civil and Environmental Engineering, Stanford University, Stanford, CA.

[27] Mehanny S. and Deierlein G.G., 2000. Assessing seismic performance of composite (RCS) and steel moment framed buildings. *Proceedings of the Twelth World Conference on Earthquake Engineering*, Auckland, New Zealand.

[28] Sabetta F. and Pugliese A., 1996. Estimation of response spectra and simulation of nonstationarity earthquake ground motions. *Bulletin of the Seismological Society of America*, Vol. 86, No. 2, pp. 337-352.

[29] Shome N. and Cornell C.A., 1999. Probabilistic seismic demand analysis of nonlinear structures. *Reliability of Marine Structures Program*, Report No. RMS-35, Department of Civil and Environmental Engineering, Stanford University, Stanford, CA.

[30] Shome N., Cornell C.A., Bazzurro P. and Carballo J.E., 1998. Earthquakes, records, and nonlinear responses. *Earthquake Spectra*, Vol. 14, No. 3, pp. 469-500.

[31] Tothong P. and Cornell C.A., 2006. An empirical ground-motion attenuation relation for inelastic spectral displacement. *Bulletin of the Seismological Society of America*, Vol. 96, No. 6, pp. 2146-2164.

[32] Tothong P. and Luco N., 2007. Probabilistic seismic demand analysis using advanced ground motion intensity measures. *Earthquake Engineering and Structural Dynamics*, Vol. 36, No. 13, pp.1837-1860.

[33] Vamvatsikos D. and Cornell C.A., 2002. Incremental dynamic analysis. *Earthquake Engineering and Structural Dynamics*, Vol. 31, No. 3, pp. 491-514.

[34] Vamvatsikos D. and Cornell C.A., 2004. Applied incremental dynamic analysis. *Earthquake Spectra*, Vol. 20, No. 2, pp. 523-553.

[35] Wen Y.K. and Wu C.L., 2001. Uniform hazard ground motions for mid-America cities. *Earthquake Spectra*, Vol. 17, No. 2, pp. 359-384.

[36] Whittaker A., Deierlein G., Hooper J. and Merovich A., 2004. *Enginnering Demand Parameters for Structural Framing Systems*. ATC-58 Structural Performance Products Team, Redwood City, CA.

[37] Yun S.Y., Hamburger R.O., Cornell C.A. and Foutch D.A., 2002. Seismic performance evaluation for steel moment frames. *Journal of Structural Engineering*, Vol. 128, No. 4, pp.534-545.

[38] Zareian F., 2006. Simplified performance-based earthquake engineering. *Ph.D. Dissertation*, Department of Civil and Environmental Engineering, Stanford University, Stanford, CA.